Journal of Molecular and Cellular Cardiology 52 (2012) 1083–1090

Contents lists available at SciVerse ScienceDirect

Journal of Molecular and Cellular Cardiology

journal homepage: www.elsevier.com/locate/yjmcc

Original article

Regional mechanics determine collagen fiber structure in healing myocardial infarcts

Gregory M. Fomovsky [a], Andrew D. Rouillard [a], Jeffrey W. Holmes [a,b,c,*]

[a] Department of Biomedical Engineering, University of Virginia, USA
[b] Department of Medicine, University of Virginia, USA
[c] Robert M. Berne Cardiovascular Research Center, University of Virginia, USA

ARTICLE INFO

Article history:
Received 15 October 2011
Received in revised form 10 February 2012
Accepted 28 February 2012
Available online 7 March 2012

Keywords:
Agent-based modeling
Anisotropy
Fibroblast
Heart
Rat
Scar
Strain

ABSTRACT

Following myocardial infarction, the mechanical properties of the healing infarct are an important determinant of heart function and the risk of progression to heart failure. In particular, mechanical anisotropy (having different mechanical properties in different directions) in the healing infarct can preserve pump function of the heart. Based on reports of different collagen structures and mechanical properties in various animal models, we hypothesized that differences in infarct size, shape, and/or location produce different patterns of mechanical stretch that guide evolving collagen fiber structure. We tested the effects of infarct shape and location using a combined experimental and computational approach. We studied mechanics and collagen fiber structure in cryoinfarcts in 53 Sprague–Dawley rats and found that regardless of shape or orientation, cryoinfarcts near the equator of the left ventricle stretched primarily in the circumferential direction and developed circumferentially aligned collagen, while infarcts at the apex stretched similarly in the circumferential and longitudinal directions and developed randomly oriented collagen. In a computational model of infarct healing, an effect of mechanical stretch on fibroblast and collagen alignment was required to reproduce the experimental results. We conclude that mechanical environment determines collagen fiber structure in healing myocardial infarcts. Our results suggest that emerging post-infarction therapies that alter regional mechanics will also alter infarct collagen structure, offering both potential risks and novel therapeutic opportunities.

1. Introduction

Once myocardium dies during a heart attack, it is gradually replaced by scar tissue over the course of several weeks. The mechanical properties of the healing scar are a critical determinant of both depression of pump function and the eventual transition to heart failure [1]. Over a decade ago, we reported that infarcts resulting from ligation of an obtuse marginal branch of the left circumflex (LCx) coronary artery in pigs develop a structurally and mechanically anisotropic scar containing highly aligned, circumferentially oriented collagen fibers [2,3]. Considering similar reports of structural [4] and mechanical [5] anisotropy in healing canine and ovine infarcts, we were very surprised to find recently that infarcts resulting from ligation of the left coronary artery in rats develop isotropic scars containing randomly aligned collagen [6].

We recently showed that infarct anisotropy, not just overall stiffness, is an important determinant of left ventricular function in a computational model of the infarcted left ventricle [7]. Therefore, understanding what determines collagen fiber structure in healing infarcts has potentially important therapeutic applications. The infarcts we studied in pigs and rats differed in size, shape, location, and mechanical environment. Ligating an obtuse marginal of the LCx in the pig creates relatively small, elliptical infarcts oriented longitudinally on the left ventricle (LV) that do not involve the apex; these infarcts stretch circumferentially during healing [8]. By contrast, coronary ligation in the rat generates large, circular infarcts involving most of the lower half of the LV; these infarcts stretch both circumferentially and longitudinally [6]. We hypothesized that differences in infarct size, shape, and/or location produce different patterns of mechanical stretch, which then guide the evolving collagen fiber structure. In the present study, we used a combined experimental and computational approach to test the effects of infarct shape and location. We created an experimental model where we could vary infarct shape and location independently in rats using custom liquid-nitrogen-cooled cryoprobes with different tips, and examined the impact of infarct shape and location on regional mechanics and healing infarct structure. Then, we utilized a computational model of infarct healing to test whether a direct effect of regional mechanics on the orientation of fibroblasts and the collagen fibers they deposit could explain the collagen fiber structures we observed in healing cryoinfarcts.

2. Methods

2.1. Study and cryoprobe design

In order to vary infarct shape and location, we created custom cryoprobes consisting of hollow stainless steel tubes (Fig. 1; 3.75 in.

* Corresponding author at: Biomedical Engineering and Medicine, Box 800759, Health System, University of Virginia, Charlottesville, VA 22908, USA. Tel.: +1 434 243 6321; fax: +1 434 982 3870.
E-mail address: holmes@virginia.edu (J.W. Holmes).

0022-2828/$ – see front matter © 2012 Elsevier Ltd. All rights reserved.
doi:10.1016/j.yjmcc.2012.02.012

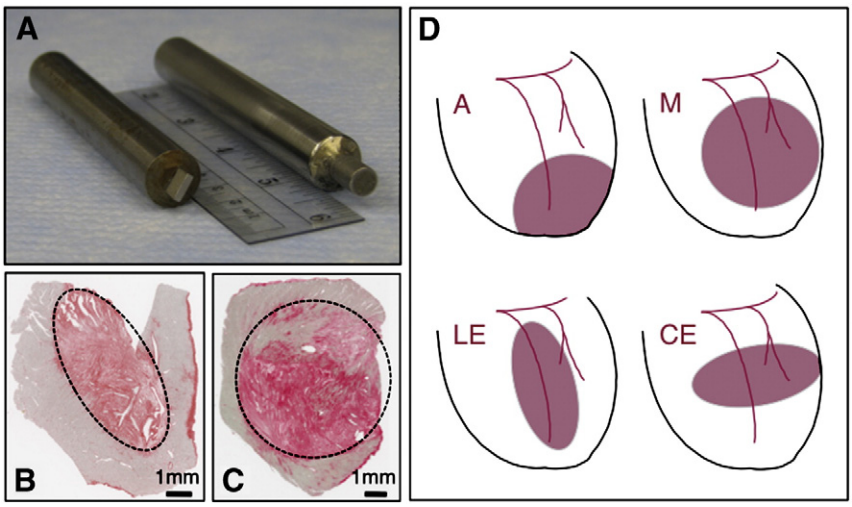

Fig. 1. Cryoinfarct methods and study design. A) Hollow steel cylinders fitted with rectangular (6.2 mm × 1.7 mm) or circular (6.4 mm diameter) porous stainless steel tips and filled with liquid nitrogen provided a tip temperature of −100 °C for 1 min. B, C) 45 s of contact with the heart surface produced nearly transmural elliptical (B, rectangular tip) or circular (C, circular tip) infarcts as shown by picrosirius red staining 3 weeks later; V-shaped notch in (B) and missing corners in both sections were introduced to track orientation during processing. Scale bars indicate 1 mm. D) The study compared circular cryoinfarcts at two different locations (apex, A; mid-ventricular anterior wall, M) as well as cryoinfarcts with different shapes and orientations at a single mid-ventricular location on the anterior wall (circle, M; longitudinally oriented ellipse, LE; circumferentially oriented ellipse, CE).

long, 0.5 in. inner diameter, 0.031 in. wall thickness) fitted with porous stainless steel tips (316L, Mott Corporation, Farmington, CT; rectangular tip dimensions, 6.2 mm × 1.7 mm; circular tip 6.4 mm diameter). When filled with liquid nitrogen, evaporation held the probe tip temperature at −100 °C for at least 1 min. To test the impact of infarct location, we created circular cryoinfarcts at the apex (A) and on the anterior wall at the mid-ventricle (M, Fig. 1). To test the impact of infarct shape, we created circular (M), longitudinally oriented elliptical (LE), and circumferentially oriented elliptical (CE) cryoinfarcts on the anterior wall at the mid-ventricle (Fig. 1). We performed acute, nonsurvival studies to measure the effect of cryoinfarction shape and location on infarct mechanics and parallel survival studies to measure the effect of cryoinfarction shape and location on infarct collagen structure at 3 weeks.

2.2. Surgical protocols

The University of Virginia Animal Care and Use Committee approved all studies. To assess the impact of infarct shape and location on regional mechanics, we created acute cryoinfarcts in 30 adult male Sprague–Dawley rats weighing 397 ± 64 g (M n = 7; LE n = 7; CE n = 6; A n = 6; 4 acute deaths as a result of the infarction procedure). Following anesthesia with isoflurane in 100% O_2 (5.0% induction, 2.5% maintenance) and intubation via tracheotomy, we established positive-pressure ventilation and opened the chest via midline sternotomy. We created cryoinfarcts by application of the custom cryoprobes to the heart surface for 45 s, then sewed seven sonomicrometer crystals (Sonometrics, London, Ontario, Canada) to the epicardial surface of the LV for real-time measurement of base-apex (BA) and anterior–posterior (AP) distances as well as circumferential and longitudinal segment lengths within the infarct region (acquisition at 312 Hz using SonoLAB software, Sonometrics). A Millar SP-671 pressure transducer (Millar Instruments, Houston, Texas) inserted into the LV cavity through the anterior wall measured LV pressure. Temporary occlusions of the inferior vena cava (IVC) and aorta (Ao) performed 45 min after infarction allowed assessment of LV pump function and infarct mechanics over a range of loading conditions. For comparison, we report here regional mechanics following coronary ligation in 6 rats measured using the same methods and reported previously [6]. Following cardiac arrest by retrograde aortic perfusion with cold 2,3-butanedione monoxime (BDM, Sigma Biochemicals, St. Louis, MO) in phosphate-buffered saline (PBS), we assessed transmural penetration of the cryoinjury by incubating short-axis slices of the LV for 15 min at 37 °C in 0.1% Nitroblue Tetrazolium (NBT) in 0.1 M Sorensen's Phosphate Buffer.

To assess the impact of infarct shape and location on collagen fiber structure in healing infarct scars, we created cryoinfarcts in 52 adult male Sprague–Dawley rats weighing 344 ± 24 g (M n = 6; LE n = 7; CE n = 7; A n = 7; 25 perioperative deaths, with an unexpectedly high mortality rate of >70% in the M group). Following anesthesia with an intraperitoneal injection of ketamine (80 mg/kg) and xylazine (5 mg/kg), intubation, and establishment of positive-pressure ventilation with room air, we performed a left thoracotomy, opened the pericardium, and applied a cryoprobe to the LV surface for 45 s; we sprayed sterile, room-temperature saline onto the tip of the cryoprobe to facilitate its detachment from the epicardial surface. We then closed the chest in layers, injected bupivacaine (2.5 mg/kg) near the incision site and administered subcutaneous buprenorphine (0.05 mg/kg) for postoperative pain, with additional injections of buprenorphine every 12 h for the first 48 h. Three weeks after cryoinfarction, we harvested hearts under deep anesthesia for histological analysis of scar collagen fiber structure as outlined below.

2.3. Regional strain analysis

Using custom algorithms written in MATLAB (v7.0, The Mathworks, Natick, MA), we computed LV volumes and infarct strains from sonomicrometry as follows. Assuming the rat left ventricle is a truncated ellipse with circular cross-section, we calculated the volume enclosed by the epicardial surface from anterior–posterior (AP) and base-apex (BA) segment lengths as: (derived in Holmes 2004 [9] based on Eq. (20) in Streeter and Hanna 1973 [10])

$$V = 1.125(\pi/6)AP^2\ BA \tag{1}$$

We measured LV mass post-mortem in each animal, computed wall volume assuming a myocardial density of 1.06 g/cm^3, and subtracted wall volume from epicardial volume to obtain cavity volume [9]. We used computed cavity volumes and measured pressures to identify end diastole (ED) as the point immediately preceding the sharp rise in pressure and end systole (ES) as the point of maximal elastance [9].

We computed strains reflecting regional deformation in the infarct region between ED and ES from segment lengths measured by sonomicrometry as described previously by Villarreal et al. [11]. Assuming that strain is locally homogeneous, the Lagrangian strain tensor **E** describes how a vector d**X** oriented in any direction will deform. Changes in the length of that vector can be computed from:

$$ds^2 - dS^2 = d\mathbf{X}^T \ \mathbf{E} \ d\mathbf{X}, \quad (2)$$

where ds^2 is the squared deformed segment length and dS^2 is the squared undeformed length. The four crystals sewed to the epicardial surface of the infarct provided up to six segment lengths at each time point (a minimum of three are needed to compute two-dimensional strains), and digitizing the positions of the crystals from images taken in the relaxed, arrested state immediately following the study provided the orientation of each segment relative to the circumferential and longitudinal directions on the heart. Given ds^2, dS^2, and d**X** values for at least three segments, solving Eq. (2) for **E** yielded circumferential (E_{CC}), longitudinal (E_{LL}), and shear strain (E_{LC}) components. Reported values represent averages over 3–5 consecutive heart beats.

2.4. Histology and structural analysis

Following arrest, we dissected 3-week scars, fixed them unloaded in 3.7% formaldehyde in phosphate-buffered saline (PBS), embedded them in paraffin, sectioned them parallel to the epicardial surface at 7 μm thickness, stained them with picrosirius red (PSR), and quantified collagen orientation using polarized light methods modified from Whittaker [12] and described in detail in our recent report of infarct structure following coronary ligation in the rat [6]. Briefly, digital image subtraction of bright-field from circularly polarized images isolates collagen, the only tissue component that is bright under polarized light but dark red under brightfield illumination of PSR-stained sections, and automated analysis of the resulting image provides a histogram of collagen fiber orientation for each image.

Applying a cryoprobe to the epicardial surface of a beating heart produced conical cryoinfarcts, largest at the epicardial surface, with the tip just reaching the endocardial surface. To minimize confounding effects of transmural variations in mechanics, healing, and structure, we analyzed sections 30% of the distance from epicardium to endocardium in all animals. For each section, we selected 10 fields at 10× magnification (0.48×0.36 mm region of the section) using a standardized sampling grid and averaged the resulting orientation histograms to obtain a single histogram for each scar. We utilized circular statistics for analysis, representing angles as unit vectors and performing averaging and other calculations on vector components [13]. We tested for the presence of significant alignment by testing whether the dot products of a group of vectors with their mean vector were different from 0 by a one-sample *t*-test [14].

2.5. Computational model

Motivated by previous work using agent-based models to explore the role of chemotaxis in skin wound healing [15], we created an agent-based model of fibroblast migration and collagen deposition in healing infarcts. The computational model represented fibroblasts as individual disk-shaped "agents" that were free to move about a 2-dimensional spatial domain. We represented infarcts as regions initially free of fibroblasts but generating chemokines reflecting inflammation that attracted fibroblasts into the infarct from the surrounding myocardium. Fibroblasts migrated, proliferated, and degraded matrix at rates proportional to local chemokine concentration and underwent apoptosis when they reached a finite lifetime. For each cell, at each time step, a weighted vector average of the directional cues in the local environment – stretch (mechanotaxis), chemokine concentration gradient (chemotaxis), fiber structure (contact guidance), and current cell direction (persistence) – provided a resultant vector that guided migration, the orientation of newly deposited collagen fibers, and rotation of existing collagen fibers by that cell. The model contained a total of 19 variable parameters; 9 were specified directly from published *in vitro* studies on fibroblasts and 5 were determined by simulating published experiments. Migration parameters were chosen to match published *in vitro* migration data in collagen gels with varying matrix alignment [16]. The initial collagen content and matrix alignment were assumed to be the same as that measured in healthy rat myocardium, and the rates of collagen deposition and degradation were chosen to match collagen-content vs. time data from Fomovsky [6]. Of the remaining 5 parameters not directly available from literature, only 3 affected model predictions of collagen alignment: the weighting factors for the contributions of mechanical and chemical cues, which were set equal to the weighting factor for contact guidance, and the rate of collagen fiber rotation, which was estimated from our own measurements of the rate of collagen gel compaction by cardiac fibroblasts. Using this model, we examined the effects of infarct shape, pre-existing extracellular matrix orientation, and mechanical stretch on scar collagen fiber structure at 3 weeks of simulated healing.

3. Results

3.1. Effect of infarct shape and location on regional mechanics

Regional systolic deformation varied with location on the LV, and was independent of the shape of the infarcted region (Fig. 2). Acute cryoinfarcts located near the equator on the anterior wall of the LV all stretched uniaxially in the circumferential direction, regardless of shape (CE, LE, M); strains in these infarcts were similar to those we reported previously in pigs [8]. By contrast, acute circular cryoinfarcts that involved the LV apex (A) stretched significantly in both the circumferential and longitudinal directions, similar to acute rat infarcts created by coronary ligation [6].

3.2. Effect of infarct shape and location on scar collagen structure

Collagen fiber alignment in 3-week cryoinfarct scars varied with the location on the LV, and was independent of the shape of the infarcted region (Fig. 3, Table 1). Cryoinfarcts located near the equator on the anterior wall of the LV all developed significant collagen fiber

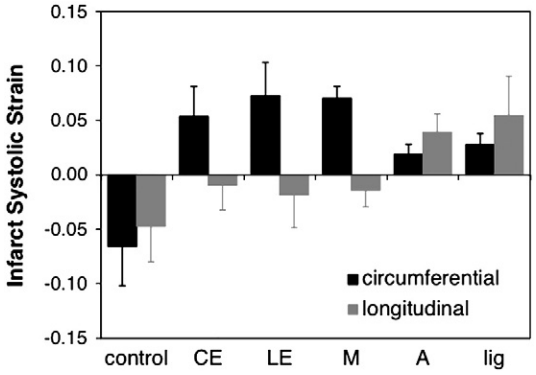

Fig. 2. Acute regional mechanics following cryoinfarction. Acute cryoinfarcts located near the equator on the anterior wall of the LV all stretched uniaxially in the circumferential direction, regardless of shape (CE, LE, M). By contrast, acute circular cryoinfarcts that involved the LV apex (A) stretched significantly in both the circumferential and longitudinal directions, similar to acute infarcts created by coronary ligation (lig). CE—circumferentially oriented, elliptical cryoinfarct at the midventricle; LE—longitudinally oriented, elliptical cryoinfarct at the midventricle; M—circular cryoinfarct at the midventricle on the anterior wall; A—circular cryoinfarct at the apex; lig—coronary ligation.

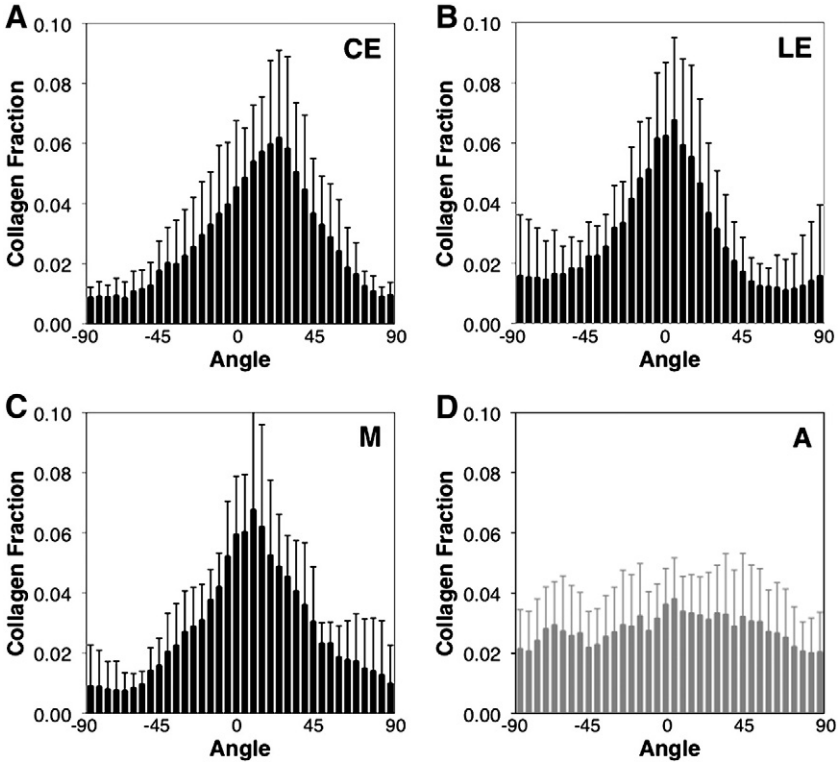

Fig. 3. Collagen orientation histograms 3 weeks after cryoinfarction. A–C) Cryoinfarcts located near the equator on the anterior wall of the LV all developed significant collagen fiber alignment in the circumferential direction. D) By contrast, circular cryoinfarcts that involved the LV apex (A) developed an isotropic collagen fiber structure, similar to 3-week scars resulting from coronary ligation in the rat [6]. CE—circumferentially oriented, elliptical cryoinfarct at the midventricle; LE—longitudinally oriented, elliptical cryoinfarct at the midventricle; M—circular cryoinfarct at the midventricle on the anterior wall; A—circular cryoinfarct at the apex.

alignment in the circumferential direction (CE, LE, M), similar to the circumferential alignment we reported previously in pigs [2,3]. By contrast, circular cryoinfarcts that involved the LV apex (A) developed an isotropic collagen fiber structure, similar to 3-week scars resulting from coronary ligation in the rat [6]. Thus, collagen fiber structure correlated with the mechanical environment in healing infarct scars, rather than with infarct shape.

3.3. Computational model

The collagen fiber distribution predicted by the model agreed closely with the measured distributions in the cryoinfarcts for all groups (shown for LE in Fig. 4B). The influence of mechanical stretch on fibroblast orientation was required for accurate predictions; when the coefficient modulating sensitivity to mechanical stretch was set to zero, predicted distributions fell outside one standard deviation of the experimental data (Fig. 4B). By contrast, pre-existing matrix orientation and infarct shape were much less critical to matching the observed distributions. The effect of the initial matrix alignment faded with time in the simulations; by 3 weeks, predicted distributions fell within one standard deviation of the measured distributions whether the matrix in the infarct region was assumed to be initially random, perfectly aligned in the circumferential direction, or (as measured in healthy myocardium) somewhere in between (Fig. 4C). Infarct shape did affect fibroblast migration into the model infarct through chemokine gradients, consistent with prior models of chemotaxis in healing skin wounds [15], but the overall impact on predicted structure was small compared to the effect of mechanics (Fig. 4D), consistent with the experimental distributions shown in Fig. 3.

Table 1
Scar size, morphology, and collagen area fraction. Morphologic and histologic analysis of tissue sections at 30% transmural depth confirmed a major:minor axis ratio of approximately 2 in elliptical infarcts and provided information on the relative size and collagen content of the various infarcts. *Data from Fomovsky [6]. All values reflect mean ± SD.

	Ligation*	M	CE	LE	A
Area (mm^2)	59.0 ± 14.4	40.3 ± 4.1	21.2 ± 9.1	24.0 ± 4.4	22.5 ± 5.4
Axis ratio	–	1.3 ± 0.01	2.1 ± 0.4	1.8 ± 0.3	–
Collagen (%)	19.4 ± 7.0	34.9 ± 7.0	26.5 ± 8.8	20.4 ± 1.7	34.9 ± 6.7

4. Discussion

We compared circular cryoinfarcts in two locations (apex, A, and mid-ventricular, M) to test the effect of infarct location; and compared circular (M), circumferentially-oriented (CE), and longitudinally-oriented elliptical (LE) infarcts all in the same mid-ventricular location to test the effect of infarct shape and orientation relative to the pre-existing tissue architecture. We found that infarct shape and orientation were irrelevant to both infarct mechanics and scar structure; to our surprise, only infarct location mattered in these experiments. Cryoinfarcts near the LV equator stretched primarily in the circumferential direction and developed anisotropic scars containing circumferentially aligned collagen fibers, just as we had reported previously in pigs. Infarcts at the apex stretched in both the circumferential and longitudinal directions, and developed structurally isotropic scars, just as we reported following coronary ligation in the rat. In a computational model of infarct healing, regulation of fibroblast and collagen fiber orientation by regional mechanics was required to explain the collagen fiber structures observed in healing cryoinfarcts, while contact guidance by pre-existing extracellular matrix and effects of infarct shape on chemotactic gradients and fibroblast migration could not explain the experimental results. Taken together, these results suggest that mechanical environment

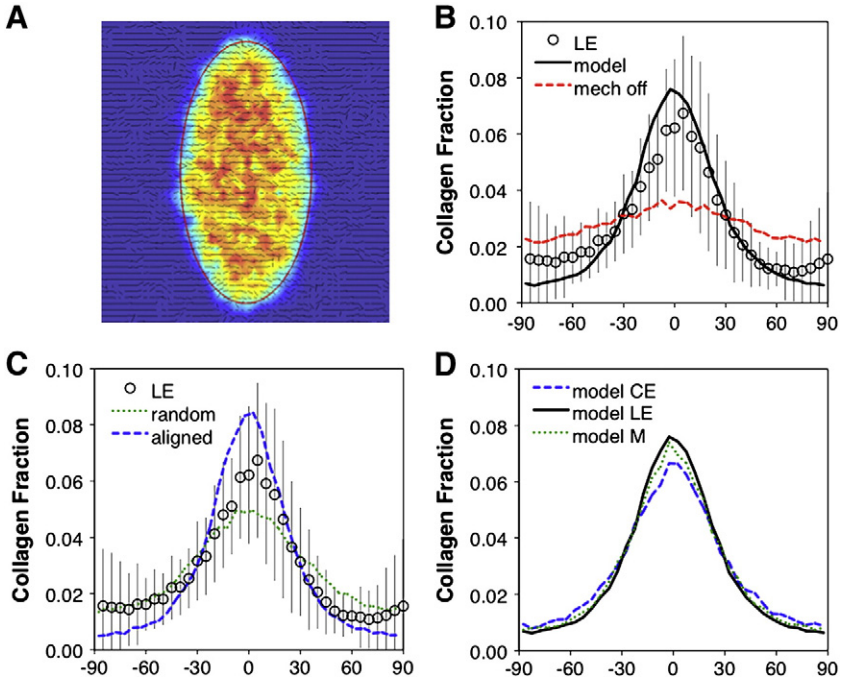

Fig. 4. Predicted collagen fiber orientations in a computational model of infarct healing. A) Model response to 3 weeks of uniaxial circumferential stretch in longitudinally oriented elliptical infarct; red line indicates infarct border, color indicates collagen density (blue lowest, red highest), and black lines indicate mean local collagen fiber direction. B) Model matched measured cryoinfarct distributions well when mechanical cues were included but not when these were turned off; error bars indicate SD. C) Model predictions fell within 1 SD of experimental mean regardless of assumed initial matrix alignment, from random to perfectly aligned in the circumferential direction. D) Infarct shape had little impact on model predictions in the presence of uniaxial stretch, consistent with experimental results; CE—circumferentially oriented ellipse; LE—longitudinally oriented ellipse; M—circular cryoinfarct; x axis of panels B-D is angle in degrees.

guides collagen fiber structure in healing infarcts and that therapies that perturb regional mechanics may also alter scar structure.

4.1. Collagen structure in healing myocardial infarcts

We report here that collagen fibers in mid-ventricular cryoinfarcts in the rat are highly aligned in the circumferential direction, while collagen fibers in apical cryoinfarcts are randomly aligned; we reported recently that collagen fibers in large anteroapical infarcts resulting from coronary ligation in rats are also randomly aligned. By contrast, Whittaker [17] and Zhou et al. [18] reported high levels of collagen fiber alignment following coronary ligation in the rat. The reason for this apparent discrepancy is the choice of different sectioning planes in these studies. As illustrated in Fig. 5, following coronary ligation in the rat, collagen is organized in planes parallel to the epicardial surface, but its orientation within each of these planes is random. When the heart is cut into short-axis cross-sections and the collagen is viewed in the circumferential–radial plane (Fig. 5A), it appears highly aligned in the circumferential direction, because most collagen fibers are parallel to the epicardial surface. However, when the same infarct is sectioned parallel to the epicardial surface, the random orientation of collagen fibers in the circumferential–longitudinal plane becomes apparent (Fig. 5B). Interestingly, Zhou also found that mechanical unloading of infarcted rat hearts by heterotopic transplantation decreased the degree of alignment in the circumferential–radial plane [18], consistent with the overall conclusions of the present study.

We focus on the circumferential–longitudinal plane in our studies because the collagen fiber orientation in this plane determines the *in situ* mechanics of the infarct and its effect on left ventricular function. When the left ventricle is pressurized, the infarct is placed under tension in the circumferential and longitudinal directions and compression in the radial direction. Because collagen fibers contribute to tissue mechanics only under tension (they buckle under compression), even fibers that are angled transmurally across the wall don't contribute much to mechanics in the radial direction. By contrast, the number of collagen fibers oriented in the circumferential vs. longitudinal directions in planes parallel to the epicardium, together with the circumferential and longitudinal wall stresses acting on the infarct, determines how much the infarct stretches in the circumferential and longitudinal directions, and this stretching (dyskinesis) is the source of LV systolic dysfunction. The mechanics are similar to other well-studied examples in cardiovascular mechanics; for example, myofiber orientations in planes parallel to the epicardial surface determine LV shape changes during filling [19,20], and the helix angle of the collagen fiber weave in the arterial wall determines the balance between circumferential and longitudinal expansion during inflation [21].

We did not directly test the effects of infarct size in this study; however, our results suggest that infarct size was not an important determinant of mechanics or structure. Circular and elliptical cryoinfarcts at the mid-ventricle had similar mechanics and structure despite a two-fold difference in area (Table 1), and circular cryoinfarcts at the apex and anteroapical infarcts resulting from coronary ligation had similar mechanics and structure despite a 50% difference in area. We also observed substantial differences in collagen area fraction in the different infarct groups (Table 1), but could not identify a clear relationship between collagen area fraction and infarct size, shape, location, or mechanics.

4.2. Regulation of collagen alignment in healing myocardial infarcts

The regulation of collagen fiber orientation by mechanical environment appears to be a general feature of wound healing in mechanically loaded tissues. As examples, collagen fibers align along the direction of applied tension in healing skin wounds but orient randomly in the absence of applied tension [22,23], and hindlimb unloading and joint immobilization affect the organization of collagen fibers in healing ligaments [24–26]. Accordingly, many recognized features of fibroblast biology could govern the alignment of collagen fibers in healing myocardial infarcts. The data and simulations

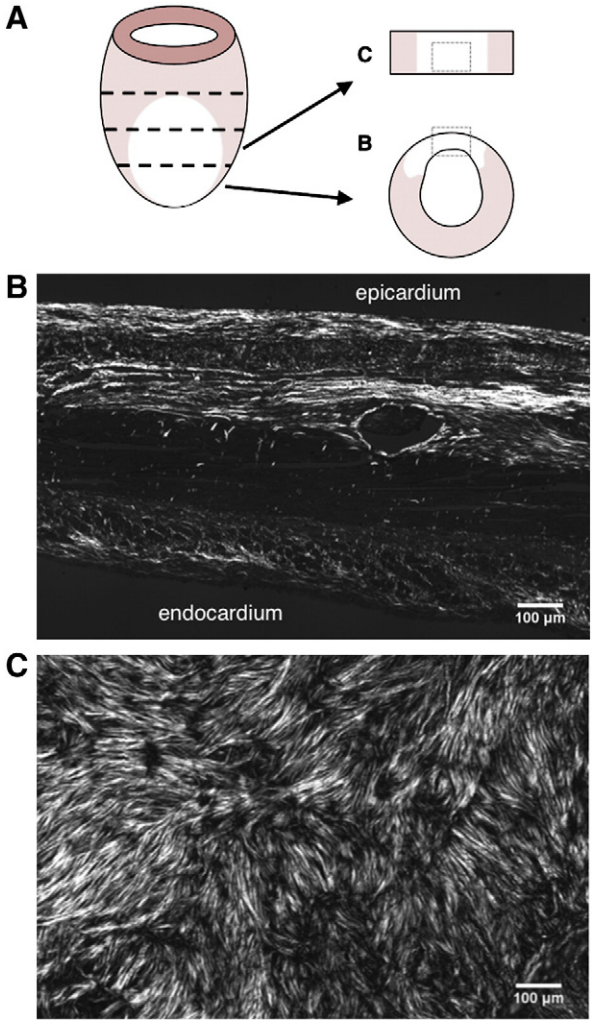

Fig. 5. Effect of sectioning plane on apparent collagen orientation 3 weeks after coronary ligation in the rat. A) Schematic showing location and orientation of sections. LV was divided into 4 transverse rings, and the apical ring sectioned perpendicular to the epicardium, starting from the basal side; dotted rectangle indicates approximate region shown in panel B. The adjacent ring was sectioned parallel to the epicardial surface, to provide another view of the same region of the infarct. B) Collagen is arranged in planes parallel to the epicardial surface; in short-axis sections of the heart, it therefore appears highly aligned in the circumferential direction. C) Sections parallel to the epicardial surface show the orientation of the collagen in the circumferential–longitudinal plane; following coronary ligation, collagen fibers are oriented randomly in this plane. Sections stained with picrosirius red and imaged through a 10× objective under circularly polarized light.

presented here allow us to exclude some of those potential mechanisms in the case of healing cryoinfarcts.

First, the inflammatory process in healing wounds generates chemokines that attract migratory cells into the wound. MacDougall et al. predicted that wound shape could influence fibroblast migration patterns and collagen fiber orientation in healing skin wounds through the effect of wound shape on local chemokine gradients [15]. We studied three groups of cryoinfarcts (M, CE, LE) with different shapes and orientations but identical locations on the left ventricle (and therefore pre-existing matrix) and mechanics. All three groups developed similar collagen fiber structures (Fig. 3), suggesting little impact of infarct shape on collagen fiber orientation. Model simulations predicted that infarct shape does influence collagen structure in the healing infarct, but that the impact of shape is minor compared to the effects of regional mechanics and pre-existing matrix orientation (Fig. 4).

Second, the well-known phenomenon of contact guidance could allow pre-existing extracellular matrix that survives the initial myocardial infarction to guide subsequent fibroblast migration, alignment, and collagen deposition [27]. Our model predicted that the influence of pre-existing matrix alignment decreases rapidly, so that by 3 weeks the model-predicted collagen fiber distribution fell within one standard deviation of experimentally measured means regardless of the initial degree of matrix alignment (random, perfectly aligned, or matched to the level of collagen fiber alignment in noninfarcted myocardium). We chose migration parameters for the model consistent with the level of contact guidance measured by Dickinson et al. in fibroblast-populated collagen gels [16]. Therefore, we conclude from the model results that contact guidance at levels consistent with published data is inadequate to explain the level of collagen fiber alignment we observed in healing cryoinfarcts.

In vitro, fibroblasts can align with applied uniaxial tension [28], rotate existing collagen fibers toward the cell axis [29,30], and deposit collagen fibers aligned with the cell axis [31–33]. Our results suggest that fibroblast-mediated alignment of collagen in response to mechanical cues is the most likely mechanism for the collagen fiber alignment we observed in healing infarcts. Cryoinfarcts that stretched primarily in the circumferential direction developed circumferentially aligned collagen fibers regardless of shape or orientation relative to pre-existing tissue structure, while apical cryoinfarcts and infarcts resulting from coronary ligation stretched in both the circumferential and longitudinal directions and developed random collagen fiber structures. In the computational model, an effect of mechanical stretch on fibroblast alignment and subsequent collagen remodeling and deposition was required in order to reproduce the collagen fiber structures we observed in all cryoinfarct groups.

Two other mechanisms that can influence collagen alignment in some settings were not investigated in this study. In engineered tissues such as fibroblast-populated collagen gels, differential compaction of existing collagen in the presence of anisotropic mechanical boundary conditions can produce net collagen alignment, even without new collagen synthesis [14,34–36]. While fibroblast-mediated compaction likely plays an important role in healing skin wounds, it is unclear whether it is an important feature of myocardial infarct healing. Recently, Ruberti and colleagues reported that mechanical stretch slows the rate of collagen fiber degradation by bacterial collagenase and MMP8 [37,38]. Their work suggests the intriguing possibility that net collagen fiber alignment in the direction of greatest stretch could evolve through continuing deposition of randomly aligned collagen coupled with selective degradation of unstretched fibers.

4.3. Mechanical regulation of collagen alignment: therapeutic implications

A number of post-infarction therapies currently under development or already in clinical use alter patterns of mechanical stretch in the healing infarct. Cardiac resynchronization therapy (CRT) is often applied in patients with prior myocardial infarction and changes the patterns of electrical activation and mechanical stretch throughout the heart [39,40]. Peri-infarct pacing, a variant of CRT with the explicit goal of altering deformation in the infarct, is already in clinical trials [41]. Other therapies intended to alter infarct deformation, such as polymer injection [42] and mechanical restraint [43], are also under development. The most important implication of our finding that mechanical stretch guides infarct structure is that therapies that alter infarct mechanics will also alter infarct structure, and should be designed and tested with attention to their long-term effects on infarct healing.

Taken together with a recent modeling study, our results also suggest that there is an opportunity to develop novel therapeutic interventions that guide evolving collagen fiber structure by controlling the infarct mechanical environment during healing. Using a finite-element model of large anteroapical infarcts in dogs, we found that infarcts that are much stiffer in the longitudinal direction than in

other directions provide better predicted pump function than infarcts that are stiffer in the circumferential direction or isotropically stiff [7]. Yet to our knowledge no study has ever reported longitudinally aligned collagen fibers in a healing infarct. Taken together, these two results suggest that the infarct structure that develops normally does not provide the best possible pump function, raising the possibility that manipulating the evolving infarct structure could be a novel approach to improving cardiac function following infarction.

4.4. Limitations and sources of error

We measured strains at the epicardial surface in anesthetized, open-chest rats, so the magnitude of the strains reported here is fairly small. However, the trends we observed regarding the isotropy or anisotropy of regional deformation are consistent with reported three-dimensional strain measurements at comparable locations on the heart in closed-chest patients and animals. As examples, we previously reported stretching in only the circumferential direction in 3-week infarcts in closed-chest pigs using biplane cineradiography (midwall E_{CC} 0.07 ± 0.08, E_{LL} -0.03 ± 0.05) [3], consistent with the strains reported here for the LE group; Bogaert et al. reported strains measured with MRI tagging during the first week after infarction in patients with anterior MI and found circumferential and longitudinal strains of similar magnitude at both the epicardium and endocardium [44], consistent with the A group in this study; and using MRI tagging in mice with large anterior infarcts, Young et al. reported strains of similar magnitudes at the apex but more positive circumferential strains at the mid-ventricle [45].

Because we measured strains only at the epicardial surface, we might have missed transmural strain variations. However, three-dimensional studies of infarct mechanics in larger animals have shown that circumferential and longitudinal strains become transmurally uniform within the first 5 min of ischemia [46] and remain transmurally uniform for at least 3 weeks [8], suggesting that transmural strain variations are not a prominent feature of healing infarcts. Nevertheless, transmural strain variations could have been present in this study because the cryoinfarcts are conical, decreasing in area from the epicardium to the endocardium, which raises the possibility that preserved endocardium could influence mechanics in the inner wall.

Our structural measurements focused on a single transmural depth of 30%. Consistent with mechanics studies showing little transmural strain variation, our prior studies of healing pig [3] and rat [6] infarcts showed only modest transmural variation in collagen content and alignment. Due to the conical shape of the cryoinfarcts in the present study, we were concerned that transmural variations could be more significant in the present study. We therefore repeated our structural analysis at 9 equally spaced transmural depths in the M group and found that collagen content was uniform across the entire wall, while mean collagen fiber angle remained near zero (circumferential) and degree of alignment uniform in the outer half of the wall, before shifting toward the surrounding muscle fiber direction near the endocardium.

We focused our strain measurements and structural analysis on the center of the infarct region, intentionally avoiding the border zone. While the structural transition and integration between the infarct and surrounding myocardium at the border is an important and interesting problem, the mechanics of the border are complex, making it much more difficult to directly measure gross deformation and relate it to scar structure as we were able to do in the center of the infarct. Finally, the mechanism of cell death and spatial uniformity of damage differ between cryoinfarcts and ligation-induced infarcts, although in other respects the cryoinfarcts are similar to reperfused infarcts [47]. Nevertheless, we detected clear differences between the mechanics of cryoinfarcts at the midventricle and the apex and these differences led to striking differences in collagen fiber structure at 3 weeks.

5. Conclusions

We used a combined experimental and computational approach to test the hypothesis that differences in infarct shape or location produce different patterns of mechanical stretch that guide evolving collagen fiber structure. We found that regardless of shape or orientation, cryoinfarcts near the equator of the rat ventricle stretched primarily in the circumferential direction and developed circumferentially aligned collagen, while infarcts at the apex stretched similarly in the circumferential and longitudinal directions and developed randomly oriented collagen. In a computational model of infarct healing, regulation of fibroblast and collagen fiber orientation by regional mechanics was required to reproduce the experimental results. We conclude that mechanical environment determines collagen fiber structure in healing myocardial infarcts. Based on these results, we would expect emerging post-infarction therapies that alter regional mechanics to also alter infarct collagen structure, a potential risk of these therapies that has not been considered. The ability to guide and predict evolving infarct structure by altering regional mechanics may also present new potential opportunities for therapeutic intervention.

Funding sources

This work was funded by the NIH/NHLBI R01 HL-075639 (JWH).

Disclosures

None.

Acknowledgments

The authors wish to acknowledge Dezba Coughlin Ph.D. for her assistance in designing the cryoprobes used in this study.

References

[1] Holmes JW, Borg TK, Covell JW. Structure and mechanics of healing myocardial infarcts. Annu Rev Biomed Eng 2005;7:223–53.
[2] Holmes JW, Covell JW. Collagen fiber orientation in myocardial scar tissue. Cardiovasc Pathobiol 1996;1:15–22.
[3] Holmes JW, Nunez JA, Covell JW. Functional implications of myocardial scar structure. Am J Physiol Heart Circ Physiol 1997;272:H2123–30.
[4] Whittaker P, Boughner DR, Kloner RA. Analysis of healing after myocardial infarction using polarized light microscopy. Am J Pathol 1989;134:879–93.
[5] Gupta KB, Ratcliffe MB, Fallert MA, Edmunds Jr LH, Bogen DK. Changes in passive mechanical stiffness of myocardial tissue with aneurysm formation. Circulation 1994;89(5):2315–26.
[6] Fomovsky GM, Holmes JW. Evolution of scar structure, mechanics, and ventricular function after myocardial infarction in the rat. Am J Physiol Heart Circ Physiol 2010;298(1):H221–8.
[7] Fomovsky GM, Macadangdang JR, Ailawadi G, Holmes JW. Model-based design of mechanical therapies for myocardial infarction. J Cardiovasc Transl Res 2011;4(1):82–91.
[8] Holmes JW, Yamashita H, Waldman LK, Covell JW. Scar remodeling and transmural deformation after infarction in the pig. Circulation 1994;90(1):411–20.
[9] Holmes JW. Candidate mechanical stimuli for hypertrophy during volume overload. J Appl Physiol 2004;97(4):1453–60.
[10] Streeter Jr DD, Hanna WT. Engineering mechanics for successive states in canine left ventricular myocardium. I. Cavity and wall geometry. Circ Res 1973;33(6):639–55.
[11] Villarreal FJ, Waldman LK, Lew WYW. Technique for measuring regional two-dimensional finite strains in canine left ventricle. Circ Res 1988;62(4):711–21.
[12] Whittaker P, Kloner RA, Boughner DR, Pickering GJ. Quantitative assessment of myocardial collagen with picrosirius red staining and circularly polarized light. Basic Res Cardiol 1994;89:397–410.
[13] Batschelet E. Circular statistics in biology. London: Academic Press; 1981.
[14] Thomopoulos S, Fomovsky GM, Holmes JW. The development of structural and mechanical anisotropy in fibroblast populated collagen gels. J Biomech Eng 2005;127(5):742–50.
[15] McDougall S, Dallon J, Sherratt J, Maini P. Fibroblast migration and collagen deposition during dermal wound healing: mathematical modelling and clinical implications. Philos Transact A Math Phys Eng Sci 2006;364(1843):1385–405.
[16] Dickinson RB, Guido S, Tranquillo RT. Biased cell migration of fibroblasts exhibiting contact guidance in oriented collagen gels. Ann Biomed Eng 1994;22:342–56.
[17] Whittaker P. Laser-mediated reversal of cardiac expansion after myocardial infarction. Lasers Surg Med 1999;25(3):198–206.

[18] Zhou X, Yun JL, Han ZQ, Gao F, Li H, Jiang TM, et al. Postinfarction healing dynamics in the mechanically unloaded rat left ventricle. Am J Physiol Heart Circ Physiol 2011;300(5):H1863–74.
[19] Holmes JW. Determinants of left ventricular shape change during filling. J Biomech Eng 2004;126(1):98–103.
[20] Yettram AL, Beecham MC. An analytical method for the determination of along-fibre to cross-fibre elastic modulus ratio in ventricular myocardium—a feasibility study. Med Eng Phys 1998;20:103–8.
[21] Holzapfel GA, Gasser TC, Ogden RW. A new constitutive framework for arterial wall mechanics and a comparative study of material models. J Elasticity 2000;61:1–48.
[22] Arem AJ, Madden JW. Effects of stress on healing wounds: intermittent noncyclical tension. J Surg Res 1976;20:93–102.
[23] Forrester JC, Zederfeldt BH, Hayes TL, Hunt TK. Wolff's law in relation to the healing skin wound. J Trauma 1970;10(9):770–9.
[24] Frank C, MacFarlane B, Edwards P, Rangayyan R, Liu ZQ, Walsh S, et al. A quantitative analysis of matrix alignment in ligament scars: a comparison of movement versus immobilization in an immature rabbit model. J Orthop Res 1991;9(2):219–27.
[25] Gomez MA, Woo SL, Amiel D, Harwood F, Kitabayashi L, Matyas JR. The effects of increased tension on healing medial collateral ligaments. Am J Sports Med 1991;19(4):347–54.
[26] Provenzano PP, Martinez DA, Grindeland RE, Dwyer KW, Turner J, Vailas AC, et al. Hindlimb unloading alters ligament healing. J Appl Physiol 2003;94(1):314–24.
[27] Zimmerman SD, Karlon WJ, Holmes JW, Omens JH, Covell JW. Preexisting matrix is the predominant determinant of infarct scar collagen organization. Am J Physiol Heart Circ Physiol 2000;278(1):H194–200.
[28] Haston WS, Shields JM, Wilkinson PC. The orientation of fibroblasts and neutrophils on elastic substrata. Exp Cell Res 1983;146(1):117–26.
[29] Petroll WM, Ma L. Direct, dynamic assessment of cell-matrix interactions inside fibrillar collagen lattices. Cell Motil Cytoskeleton 2003;55(4):254–64.
[30] Petroll WM, Ma L, Kim A, Ly L, Vishwanath M. Dynamic assessment of fibroblast mechanical activity during Rac-induced cell spreading in 3-D culture. J Cell Physiol 2008;217(1):162–71.
[31] Birk DE, Trelstad RL. Extracellular compartments in matrix morphogenesis: collagen fibril, bundle, and lamellar formation by corneal fibroblasts. J Cell Biol 1984;99(6):2024–33.
[32] Canty EG, Starborg T, Lu Y, Humphries SM, Holmes DF, Meadows RS, et al. Actin filaments are required for fibripositor-mediated collagen fibril alignment in tendon. J Biol Chem 2006;281(50):38592–8.
[33] Kapacee Z, Richardson SH, Lu Y, Starborg T, Holmes DF, Baar K, et al. Tension is required for fibripositor formation. Matrix Biol 2008;27(4):371–5.
[34] Barocas VH, Tranquillo RT. An anisotropic biphasic theory of tissue-equivalent mechanics: the interplay among cell traction, fibrillar network deformation, fibril alignment, and cell contact guidance. J Biomech Eng 1997;119:137–45.
[35] Costa KD, Lee EJ, Holmes JW. Creating alignment and anisotropy in engineered heart tissue: the role of boundary conditions in three-dimensional cultures. Tissue Eng 2003;9(4):567–77.
[36] Lee EJ, Holmes JW, Costa KD. Remodeling of engineered tissue anisotropy in response to altered loading conditions. Ann Biomed Eng 2008;36(8):1322–34.
[37] Bhole AP, Flynn BP, Liles M, Saeidi N, Dimarzio CA, Ruberti JW. Mechanical strain enhances survivability of collagen micronetworks in the presence of collagenase: implications for load-bearing matrix growth and stability. Philos Transact A Math Phys Eng Sci 2009;367(1902):3339–62.
[38] Flynn BP, Bhole AP, Saeidi N, Liles M, Dimarzio CA, Ruberti JW. Mechanical strain stabilizes reconstituted collagen fibrils against enzymatic degradation by mammalian collagenase matrix metalloproteinase 8 (MMP-8). PLoS One 2010;5(8):e12337.
[39] Helm RH, Byrne M, Helm PA, Daya SK, Osman NF, Tunin R, et al. Three-dimensional mapping of optimal left ventricular pacing site for cardiac resynchronization. Circulation 2007;115(8):953–61.
[40] Kerckhoffs RC, McCulloch AD, Omens JH, Mulligan LJ. Effects of biventricular pacing and scar size in a computational model of the failing heart with left bundle branch block. Med Image Anal 2009;13(2):362–9.
[41] Chung ES, Dan D, Solomon SD, Bank AJ, Pastore J, Iyer A, et al. Effect of peri-infarct pacing early after myocardial infarction: results of the prevention of myocardial enlargement and dilatation post myocardial infarction study. Circ Heart Fail 2010;3(6):650–8.
[42] Christman KL, Lee RJ. Biomaterials for the treatment of myocardial infarction. J Am Coll Cardiol 2006;48(5):907–13.
[43] Gorman RC, Jackson BM, Burdick JA, Gorman JH. Infarct restraint to limit adverse ventricular remodeling. J Cardiovasc Transl Res 2011;4(1):73–81.
[44] Bogaert J, Bosmans H, Maes A, Suetens P, Marchal G, Rademakers FE. Remote myocardial dysfunction after acute anterior myocardial infarction: impact of left ventricular shape on regional function: a magnetic resonance myocardial tagging study. J Am Coll Cardiol 2000;35(6):1525–34.
[45] Young AA, French BA, Yang Z, Cowan BR, Gilson WD, Berr SS, et al. Reperfused myocardial infarction in mice: 3D mapping of late gadolinium enhancement and strain. J Cardiovasc Magn Reson 2006;8(5):685–92.
[46] Villarreal FJ, Lew WYW, Waldman LK, Covell JW. Transmural myocardial deformation in the ischemic canine left ventricle. Circ Res 1991;68(2):368–81.
[47] van den Bos EJ, Mees BM, de Waard MC, de Crom R, Duncker DJ. A novel model of cryoinjury-induced myocardial infarction in the mouse: a comparison with coronary artery ligation. Am J Physiol Heart Circ Physiol 2005;289(3):H1291–300.